Nutrient cycling in the Indian sector of the Southern Ocean over the last 50,000 years

X. Crosta,[1] A. Shemesh,[2] J. Etourneau,[1] R. Yam,[2] I. Billy,[1] and J. J. Pichon[1,3]

Received 19 July 2004; revised 16 May 2005; accepted 23 May 2005; published 29 July 2005.

[1] Most high-southern latitude records of carbon and nitrogen isotopic ratios and elemental ratios are from the Antarctic and Polar Front zones, thus hindering a comprehensive view of nutrient cycling in the Southern Ocean. We present, for the first time, two records from the Subantarctic Zone and the southern Subtropical Zone of the Indian Ocean. These records provide a latitudinal transect covering the main oceanographic systems of the Southern Ocean. Carbon and nitrogen content of the diatom-bound organic matter increases during the last glacial in the Antarctic and Subantarctic zones but does not show a clear climate-related signal in the Subtropical Zone. Comparison of these records with sea-surface temperatures reconstructed at the core locations and record of dust deposition over Antarctica suggests that eolian iron input possibly switched diatom physiology toward higher carbon to silica and nitrogen to silica uptake and storage south of the Subantarctic Front due to the dependency of photosynthesis on iron concentration levels. Conversely, the northernmost core was too remote from any iron source over the last 50,000 years. Antarctic diatoms therefore have the sole potential to change the nutrient content of the waters escaping from the Southern Ocean, hence providing partial support to the silicic leakage hypothesis as a potential cause of lower glacial atmospheric CO_2.

Citation: Crosta, X., A. Shemesh, J. Etourneau, R. Yam, I. Billy, and J. J. Pichon (2005), Nutrient cycling in the Indian sector of the Southern Ocean over the last 50,000 years, *Global Biogeochem. Cycles*, *19*, GB3007, doi:10.1029/2004GB002344.

1. Introduction

[2] In the context of understanding climate-related changes of atmospheric CO_2 concentrations, a new hypothesis involving the Southern Ocean has been recently proposed [*Brzezinski et al.*, 2002; *Matsumoto et al.*, 2002]. The "silicic leakage" hypothesis states that the nitrate to silicic acid ratio (NO_3^-:$Si(OH)_4$) of Subantarctic Mode Waters (SAMW) is important in controlling low latitude productivity and, as a consequence, atmospheric pCO_2. During interglacial times, NO_3^-:$Si(OH)_4$ is high and SAMW mainly supply nitrate to low latitudes favoring the development of carbonated organisms. During glacial times, NO_3^-:$Si(OH)_4$ is lower and SAMW supply more silicic acid to low-latitude biota, stimulating the growth of siliceous organisms. This decreases the $CaCO_3$ to organic carbon (C_{org}) ratio, which in turn reduces atmospheric CO_2 concentration [*Archer and Johnson*, 2000]. This hypothesis assigns a supplementary role to the Southern Ocean with respect to CO_2 and climate regulation in addition to enhanced local productivity [*Kumar et al.*, 1995], surface water stratification [*François et al.*, 1997; *Sigman and Boyle*, 2000], deep-water stratification [*Toggweiler*, 1999; *Keeling and Stephens*, 2001], and sea ice extent [*Stephens and Keeling*, 2000]. The silicic leakage hypothesis is based on a set of laboratory experiments showing that diatom NO_3^-:$Si(OH)_4$ uptake ratio increases when iron is added to the medium [*Brzezinski et al.*, 2002], on a model run demonstrating that excess silica into Subantarctic waters boosts diatom growth and CO_2 drawdown [*Matsumoto et al.*, 2002], on modern oceanography indicating that SAMW supplies 75% of the nutrients necessary to the biota north of 30°S [*Sarmiento et al.*, 2004] and on the anti-correlation between records of $\delta^{15}N$ and $\delta^{30}Si$ in the Antarctic Zone that argues for a greater NO_3^- uptake and a smaller $Si(OH)_4$ uptake during glacial times [*Brzezinski et al.*, 2002]. Here we combine these findings with three down-core records of C and N isotopic and elemental ratios in three different oceanic regimes of the Southern ocean, including the modern formation zone of the SAMW [*Belkin and Gordon*, 1996; *Sarmiento et al.*, 2004], to give a larger view of nutrient cycling and to test the silicic leakage hypothesis. Our records provide a preliminary rationale to explain how nutrient ratios in the SAMW changed during the last glacial-interglacial cycle, potentially lowering atmospheric pCO_2 during cold periods.

2. Material and Methods

2.1. Material and Stratigraphy

[3] Gravity core SO136-111 (56°40′S–160°14′E, water depth 3912 m) was retrieved during the TASQWA cruise from the Emerald Basin, in the East Indian sector of the

[1]Département de Géologie et Océanographie (DGO), UMR-CNRS, Université Bordeaux I, Talence, France.
[2]Environmental Sciences and Energy Research, Weizmann Institute of Science, Rehovot, Israel.
[3]Deceased 9 November 2003.

Copyright 2005 by the American Geophysical Union.
0886-6236/05/2004GB002344

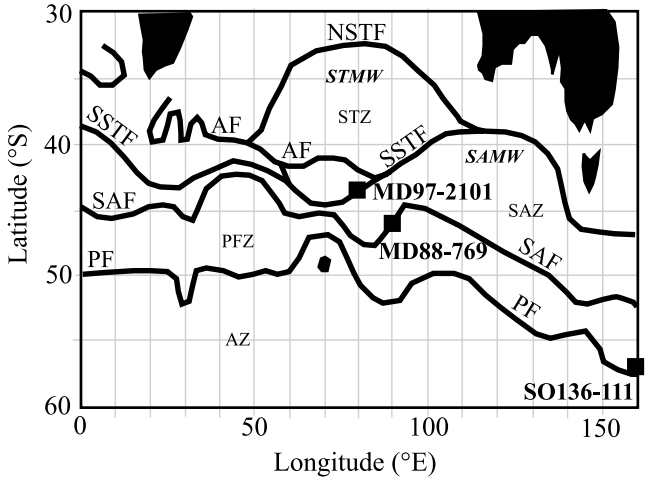

Figure 1. Core locations in three different oceanographic systems within the Indian Southern Ocean. Antarctic Zone (AZ) represents the region south of the Antarctic Polar Front (APF). Polar Front Zone (PFZ) represents the region encompassed by the APF to the south and the Subantarctic Front (SAF) to the north. Subantarctic Zone (SAZ) represents the region lying between the SAF and the southern Subtropical Front (SSTF). Subtropical Zone (STZ) represents the region north of the SSTF. SAMW, Subantarctic Mode Waters; STMW, Subtropical Mode Waters; AF, Agulhas Front. After *Belkin and Gordon* [1996].

Southern Ocean. The core is located at the position of the modern Antarctic Polar Front (APF), (Figure 1), a site representative of high surface water concentrations of nitrate and silicic acid typical of Antarctic waters [*Sarmiento et al.*, 2004]. Piston core MD88-769 (46°04′S–90°06′E, water depth 3400 m) was retrieved during the APSARA cruise on the western flank of the South East Indian Ridge at the location of the modern Subantarctic Front (SAF) (Figure 1). The core site is representative of intermediate levels of nitrate and low levels of silicic acid typical of the Subantarctic Zone [*Sarmiento et al.*, 2004]. Piston core MD97-2101 (43°30′S–79°50′E, water depth 3200 m) was retrieved during the IPHIS cruise on the western flank of the South East Indian Ridge at the location of the modern southern Subtropical Front (SSTF) (Figure 1). It is representative of low to intermediate levels of nitrate and low levels of silicic acid typical of the Subtropical Zone [*Sarmiento et al.*, 2004]. The two latter cores are located in the formation zone of the Subantarctic Mode Waters [*Belkin and Gordon*, 1996; *Sarmiento et al.*, 2004] (Figure 1).

[4] Stratigraphy of core SO136-111 is based on four AMS-^{14}C dates. Radiocarbon ages were obtained from monospecific samples of *Neogloboquadrina pachyderma* (sinistral) at the Leibniz-Labor for Radiometric Dating and Isotope Research (Germany) and were converted to calendar years using CALIB4.3 [*Stuivert et al.*, 1998] after applying a reservoir age of 800 years (Table 1). Stratigraphy of core MD88-769 is based on 13 AMS-^{14}C dates. Radiocarbon dates were obtained from monospecific samples of *Globigerina bulloides* at Gif sur Yvette (France). Radiocarbon ages were then converted to calendar years using CALIB4.3 [*Stuivert et al.*, 1998] and Bard's polynome [*Bard et al.*, 1998], after applying a reservoir age of 800 years (Table 1). Stratigraphy of core MD97-2101 is based on six AMS-^{14}C dates. Radiocarbon ages were obtained from monospecific samples of *Neogloboquadrina pachyderma* (sinistral) at the Leibniz-Labor for Radiometric Dating and Isotope Research (Germany) and were converted to calendar years using CALIB4.3 [*Stuivert et al.*, 1998] and Bard's polynome [*Bard et al.*, 1998], after applying a reservoir age of 400 years (Table 1).

2.2. Sea-Surface Temperatures and Sea Ice Estimates

[5] Diatom analysis, sediment treatment and slide preparation followed the technique described by *Rathburn et al.* [1997]. Diatom counts followed the procedures described by *Schrader and Gersonde* [1978] and *Laws* [1983]. Diatoms were taxonomically identified every 2 to 10 cm resulting in a secular to millenial resolution of the records (Figure 2). February SSTs and sea ice cover reconstructions were subsequently estimated by applying the Modern Analog Technique (MAT) to fossil diatom assemblages. Modern February SST values were collected from the World Ocean Atlas [*Levitus*, 1994] and modern values of sea ice from the *Naval Oceanography Command Detachment* [1985]. Quantitative estimates of SSTs and sea-ice duration were determined using the MAT$_5$201/31 transfer function described by *Crosta et al.* [2004]. The reconstruction of modern SST distribution and sea-ice duration by MAT$_5$201/

Table 1. Accelerator Mass Spectrometry ^{14}C Ages From Core SO136-111, MD88-769, and MD97-2101[a]

Depth, cmbsf	Age (^{14}C yr B.P) ±1 σ	1 σ on Calibration (cal yr B.P.)	Values Used in Age Model (cal yr B.P.)	Method
		SO136-111 (Reservoir Age = 800 Years)		
1	3715 ± 50	3241–3076	3163	Stuivert
31	10,235 ± 60	10,781–10,352	10,414	Stuivert
56	16,860 ± 100	19,375–18,845	19,045	Stuivert
111	43,120 ± 1870		42,320	uncalibrated
		MD88-769 (Reservoir Age = 800 Years)		
0	6180 ± 70	6272– 6152	6193	Stuivert
10	7460 ± 80	7603–7468	7553	Stuivert
20	8920 ± 80	9264–8913	8970	Stuivert
25	10,490 ± 90	11,160–10,848	10,911	Stuivert
35	12,090 ± 90	13,740–13,023	13,154	Stuivert
40	13,350 ± 120	15,337–14,188	14,720	Stuivert
82	15,400 ± 140	17,667–17,078	17,365	Stuivert
117	19,760 ± 180	22,798–21,987	22,382	Stuivert
152	23,520 ± 210		26,740	Bard
202	29,340 ± 310		33,346	Bard
212	31,770 ± 420		36,044	Bard
232	32,800 ± 470		37,177	Bard
242	34,500 ± 500		39,033	Bard
		MD97-2101 (Reservoir Age = 400 Years)		
10	4845 ± 35	5243–5047	5154	Stuivert
30	7150 ± 40	7652–7576	7608	Stuivert
80	13,480 ± 70	15,842–15,409	15,608	Stuivert
150	18,650 ± 110	21,924–21,216	21,565	Stuivert
180	30,420 ± 380		34,994	Bard
240	44,340 +2310/ −1790		43,940	uncalibrated

[a]Calendar ages were linearly interpolated between the radiocarbon dates using Analyseries software [*Paillard et al.*, 1996].

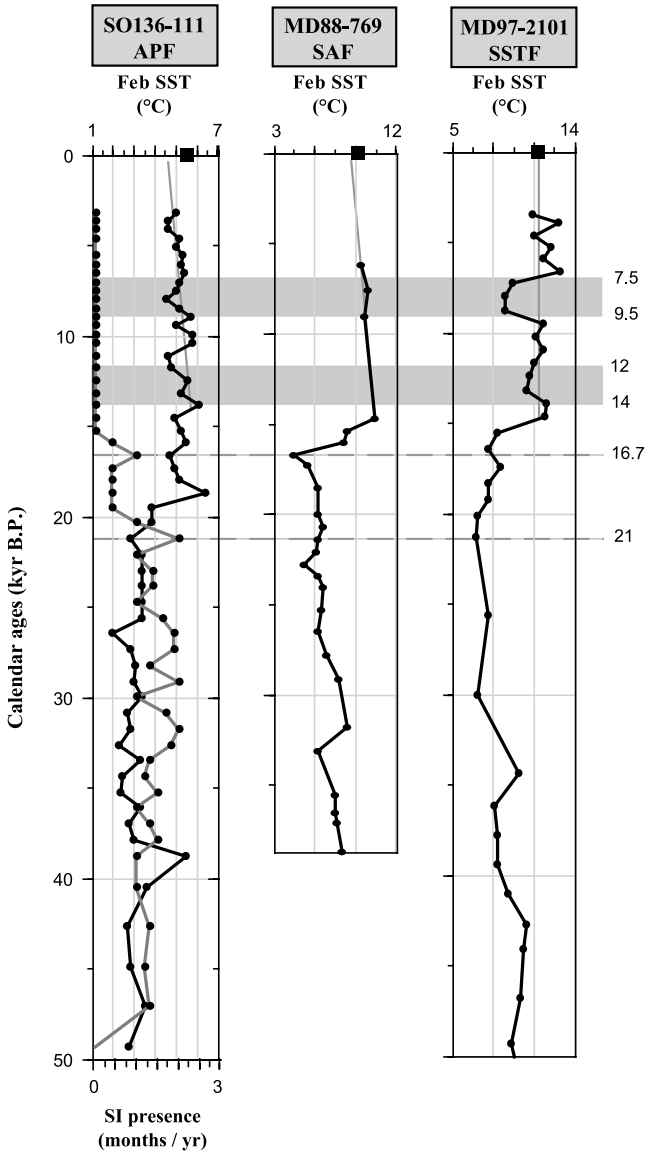

Figure 2. Down-core records of February SSTs (black line) and sea ice duration (shaded line) in cores SO136-111 (APF box), MD88-769 (SAF box), and MD97-2101 (SSTF box) as estimated by $MAT_5201/31$. Holocene trends are illustrated by thin shaded lines. Black squares represent modern February SST at the core locations [*Levitus*, 1994]. Feb SST, February sea-surface temperatures in °C; SI presence, sea ice presence in months per year.

31 produces a correlation coefficient, a mean standard error of the estimate, and a mean residual of 0.96, 0.95, and 0.75 for February SSTs and 0.99, 0.35, and 0.3 for sea-ice cover. More details about slide preparation, diatom identification and statistical treatment are given by *Crosta et al.* [2004].

2.3. Isotopes and Elemental Ratios

[6] Diatom-bound organic matter was analyzed every 5 to 10 cm for carbon and nitrogen isotopic and elemental composition, resulting in a millennial scale resolution of the records. For cores SO136-111 and MD97-2101, the cleaning procedure to isolate diatom-bound organic matter followed *Singer and Shemesh* [1995] and *Crosta and Shemesh* [2002]. We used stepwise physical washing and sieving in order to separate the diatom fraction from the bulk sediment. We then applied a perchloric/nitric oxidation to the diatom fraction <20 μm to remove the labile organic matter coating the diatom valves. Time-dependent oxidation experiments have proved that this leaching does not alter the N isotopic composition of the diatoms [*Crosta et al.*, 2002]. For core MD88-769, the cleaning procedure was changed by leaching the diatom fraction <32 μm with a hydrochloric/peroxide solution.

[7] For cores SO136-111 and MD97-2101, isotopic measurements of the acid cleaned diatoms were performed on a Carlo Erba EA1110 elemental analyzer in line with a Finnigan MAT252 stable isotope ratio mass spectrometer at the Weizmann Institute of Science (Israel). For core MD88-769, isotopic measurements were performed on a Carlo Erba 2500 elemental analyzer in line with a VG Isoprime at UMR EPOC (France). Carbon isotopes ($\delta^{13}C_{diat}$) and nitrogen isotopes ($\delta^{15}N_{diat}$) were simultaneously measured during sample combustion by peak jumping. At least two duplicates were measured for each sample. The mean standard deviations are 0.15‰ for the $\delta^{13}C_{diat}$ and 0.25‰ for the $\delta^{15}N_{diat}$. All results are reported in δ notation versus PDB for carbon and versus air for nitrogen. Internal consistency was continuously checked using several calibrated laboratory standards such as Acetanilid, Glycine and Casein. Diatom-bound C and N content of the siliceous samples were measured simultaneously with the isotopic ratios by integrating the voltage of the main ion beam. The mean standard deviations of the carbon content (C_{diat}) and the nitrogen content (N_{diat}) are ±0.018% and ±0.009%, respectively.

2.4. Nitrogen Isotopes and Cleaning Techniques

[8] Application of a different cleaning method for DIOM isotope analysis (wet chemical oxidation step combined with a denitrifier step) yields a different picture of nutrient utilization in the glacial Antarctic Zone [*Robinson et al.*, 2004] than previously evidenced [*Sigman et al.*, 1999; *Crosta and Shemesh*, 2002; *Shemesh et al.*, 2002]. The $\delta^{15}N_{diat}$ then shows very little glacial-interglacial changes with the new technique, which is at odds with previous records based on traditional combustion measurements. This discrepancy is attributed to an additional atmospheric N pool adsorbed onto particles and subsequently fractionated before or during combustion [*Robinson et al.*, 2004]. On the basis of BET surface area experiments, *Robinson et al.* [2004] state that 1 g of diatom material may held a maximum of 20–40 μmol of atmospheric N. As only 10–25% of adsorbed atmospheric N may resist the purge in the elemental analyzer, only 2–10 μmol are left as potential contaminant. N_{diat} is around 0.05% which means that 1 g of diatom material contains 36 μmol of organic N. The proportion of atmospheric N therefore represents 6–28%. Although 28% represents a potential contamination source, we doubt that this much contamination would be likely because it would imply that the whole diatom surfaces are clogged with atmospheric N and that the purge in the elemental analyzer is ineffective. It is more likely that the discrepancy between the two

methods is related to uncontrolled processes occurring during the wet chemical oxidation, hence forming compounds other than NO_3^-. Additional work is necessary at each step of the persulfate-denitrifier method to confirm the initial results of *Robinson et al.* [2004]. Until that stage, the traditional combustion method most likely represents the best technique for measuring $\delta^{15}N$ of DIOM and bulk sediment.

3. Results

3.1. Sea Ice and Sea-Surface Temperatures

[9] Modern Analog Technique (MAT) applied to fossil diatom assemblages estimates between 1 and 2 months of sea ice presence at core site SO136-111 during the last glacial period (Figure 2, APF box, shaded line). At 21 kyr B.P., maximum sea ice duration is found to be 2.1 months per year in the eastern Indian region of the Southern Ocean. Sea ice rapidly vanishes from the core site in less than 2 kyr to reach a duration of 0.5 months per year at 19.5 kyr B.P. This value is not significant as it is below two sigma of the mean standard error of $MAT_5201/31$. Besides a short but significant ice event centered at 16.7 kyr B.P., sea ice failed to reach core site SO136-111 again during the Holocene.

[10] Summer sea-surface temperatures (SSTs) around 3°C were estimated by $MAT_5201/31$ at site SO136-111 during the 50–21 kyr B.P. period (Figure 2, APF box, black line). Temperatures then abruptly increased to reach an initial maximum of 6.5°C at 18.5 kyr B.P. This warming, observed from one point, was followed by a 1.5°C cooling that lasted 4.5 kyr. At 14 kyr B.P., SSTs again reached 6°C. Subsequently, SSTs follow a cooling trend of 0.1°C per thousand years to reach 5°C at 3 kyr B.P. This trend is interrupted by two cool events at 13.5–11 kyr B.P. during the deglaciation and at 9–7 kyr B.P. during the Early Holocene.

[11] Summer SSTs estimated from diatom assemblages in core MD88-769 decreased from 8°C to 6°C during the 40–26 kyr B.P. period (Figure 2, SAF box, black line). Temperatures were stable around 6°C during the last glacial period, except for two cooling events at 22.7 kyr B.P. and 16.7 kyr B.P. Deglaciation started after the second cooling event, reaching Holocene SSTs values of 10.5°C at 14.5 kyr B.P. Subsequently, SSTs followed the same Holocene cooling trend of 0.1°C per thousand years as noted for core SO136-111. The resolution of core MD88-769, however, is too low to capture the rapid events observed at site SO136-111 during the deglaciation and the Holocene.

[12] Down-core records of SSTs in core MD97-2101 reveal a decrease from 10°C to 7°C during the 50–30 kyr B.P. period (Figure 2, SSTF, black line). Sea-surface temperatures were subsequently stable around 7°C until 16.5 kyr B.P. when deglaciation started. SSTs of 11.5°C, equivalent to Holocene values, were reached at 14.5 kyr B.P. While no Holocene trend is observed in the SST record, an intense cooling of about 3°C occurred between 9.5 and 7.5 kyr B.P.

3.2. C and N Isotopes and Elemental Ratios

[13] Carbon isotopic ratios of sedimentary diatom-bound organic matter (DIOM) in core SO136-111 were 2‰ more depleted during the last glacial than during the Early Holocene (Figure 3, APF left box, black line). Isotope values vary from −25‰ during the 40–20 kyr B.P. period to −23‰ during the 50–40 kyr B.P. period and the Early Holocene. Nitrogen isotopic ratios decrease almost continually over the last 50 kyr B.P. from a value of 8.5‰ at around 40 kyr B.P. to 3‰ during the Early Holocene (Figure 3, APF left box, shaded line). The carbon content of the DIOM slowly increased from 0.3% at 50 kyr B.P. to a maximum of 0.42% at 25 kyr B.P. and then decreased back to 0.3% at 14 kyr B.P. (Figure 3, APF right box, black line). Carbon content did not change significantly during the end of the deglaciation and the Early Holocene. Hence the glacial-interglacial change in C_{diat} is 40%. The nitrogen content of the DIOM follows the same pattern as observed for the C_{diat} but with different amplitudes varying from 0.06% at 50 kyr B.P. to a maximum value of 0.13% at 25 kyr B.P. (APF, right box, shaded line). Nitrogen content then decreases to 0.08% at 14 kyr B.P. before becoming stable during the Early Holocene. The glacial-interglacial change in diatom N content is consequently 117%. As a result of different fluctuations in C and N content, the C/N ratio of the DIOM decreases from 4.5 at 50 kyr B.P. to 3.3 during the 30–20 kyr B.P. period (Figure 3, APF right box, shaded area). C/N ratios stabilize during the Early Holocene at a value of 3.8.

[14] The $\delta^{13}C_{diat}$ in the Subantarctic core MD88-769 continually decreases from −22.5‰ at 30 kyr B.P. to −24.5‰ at 10 kyr B.P. before briefly increasing again during the Early Holocene (Figure 3, SAF left box, black line). The $\delta^{15}N_{diat}$ increases from 2‰ at 30 kyr B.P. to an average value of 4‰ during the 25–13 kyr B.P. period (Figure 3, SAF left box, shaded line). Two events at 22 kyr B.P. and 16.7 kyr B.P. present heavier than average values of $\delta^{15}N_{diat}$, while an event at 18 kyr B.P. presents lighter than average values. The Early Holocene exhibits light and stable values of $\delta^{15}N_{diat}$ around 2‰. Both C and N concentrations follow a similar trend over the last 30 kyr B.P., but again with different amplitudes. C_{diat} and N_{diat} are high between 23 and 17 kyr B.P. and low during the other periods (Figure 3, SAF right box, black and shaded lines). Both records show maximum values at 22 kyr B.P. and 16.7 kyr B.P. The average C_{diat} and N_{diat} changes on the glacial-interglacial timescale are 67% and 82%, respectively. As a result, C/N ratio was lower during full glacial conditions than during Marine Isotopic Stage 3 and the early Holocene (Figure 3, SAF right box, shaded area).

[15] The $\delta^{13}C_{diat}$ in the Subtropical core MD97-2101 increases from −24.5‰ to −23.5‰ during 50–20 kyr B.P. and subsequently stabilizes at around −24‰ until 5 kyr B.P., except for a 1.5‰ depleted event between 20 and 16 kyr B.P. (Figure 3, SSTF left box, black line). The $\delta^{15}N_{diat}$ was stable at around 8‰ during the 50–26 kyr B.P. and then experienced a decrease of 4‰ over 5 kyr between 26 and 21 kyr B.P. (Figure 3, SSTF left box, shaded line). Subsequently, only minor fluctuations occurred in the $\delta^{15}N_{diat}$ record. C_{diat} varies around 0.4–0.5% throughout the whole record except for two brief

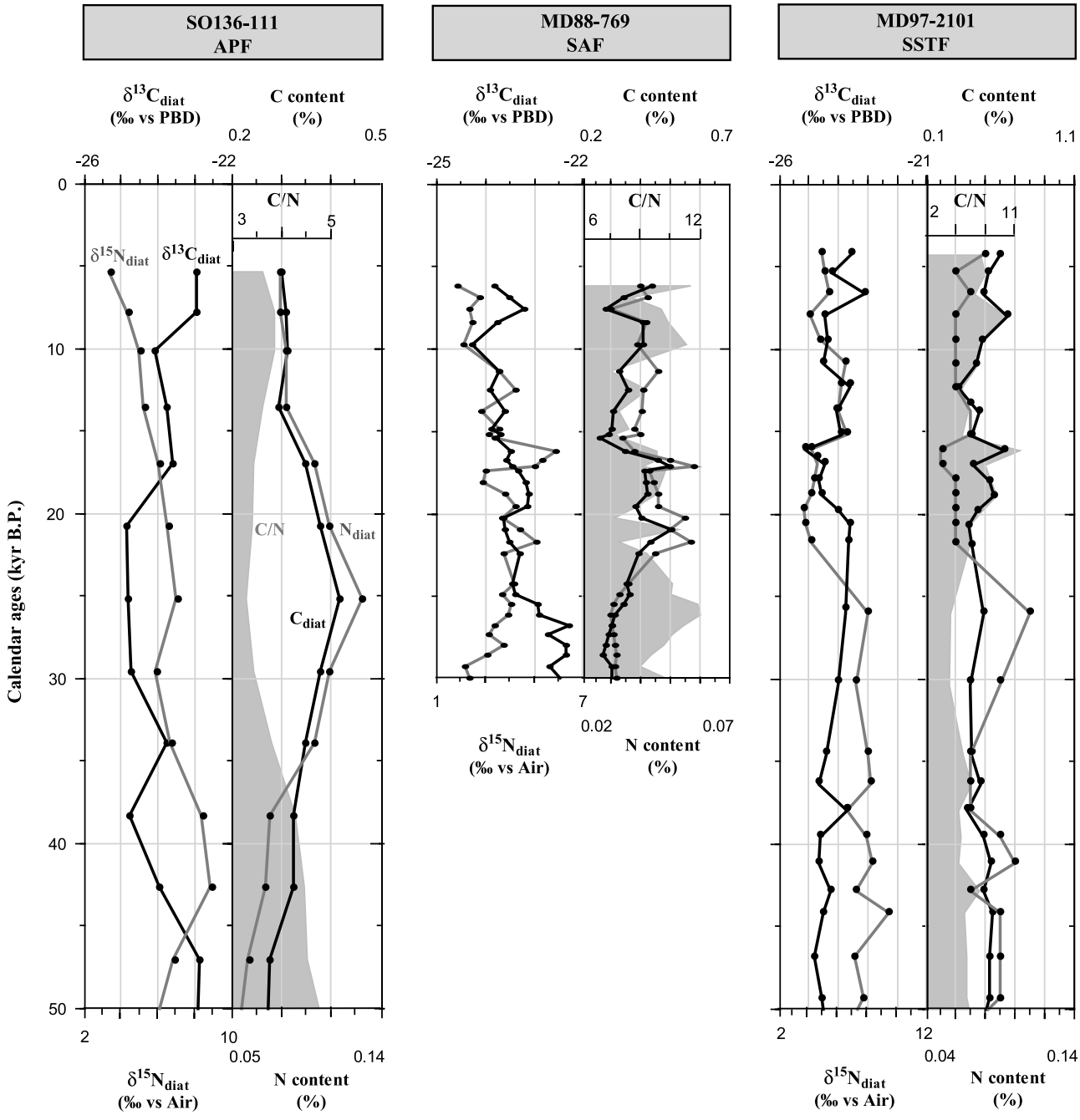

Figure 3. Down-core records of $\delta^{13}C_{diat}$ (left box, black line), $\delta^{15}N_{diat}$ (left box, shaded line), C content (right box, black line), N content (right box, shaded line) and C/N of DIOM (right box, shaded area) in cores SO136-111 (APF box), MD88-769 (SAF box), and MD97-2101 (SSTF box).

events when it reaches 0.7% at 16.5 kyr B.P. and 7.5 kyr B.P. (Figure 3, SSTF right box, black line). N averages 0.08% during the 50–26 kyr B.P. period and decreases to 0.04% in 5000 years (Figure 3, SSTF right box, shaded line). Since 21 kyr B.P., N_{diat} does not show any significant changes. As a result, C/N ratios of DIOM are relatively constant around a value of 5 during the 50–26 kyr B.P., and increases to 7 during the 21–16 kyr B.P. period and the Early Holocene when the C_{diat} increased to 0.7% (Figure 3, SSTF right box, shaded area).

4. Discussion

[16] Investigation of diatom assemblages, diatom-bound organic matter C and N isotopic and elemental ratios in three cores along a north-south transect allow SST changes

and nutrient cycling in the Subantarctic to Subtropical Zone of the Southern Ocean to be characterized. The comparison of these data sets highlights a climate-related evolution of both SST and nutrient cycling in the Antarctic and Subantarctic zones and of SST in the Subtropical Zone while nutrient cycling in the latter zone show no relationship to glacial-interglacial climate changes.

[17] Chronostratigraphically, the three cores are built upon similar age models based on radiocarbon dates. However, different ^{14}C reservoir ages may have occurred in separate regions of the Southern Ocean which in turn, may have changed through time [*van Beek et al.*, 2002] in relation to variations in sea ice cover and oceanic ventilation [*Schmittner*, 2003]. Hence core to core comparison is limited due to the dating uncertainties.

4.1. Sea-Surface Temperatures and Climate Changes

[18] The major features of the SST records are (1) less glacial cooling in the Antarctic Zone than in the Subantarctic and southern Subtropical zones with temperature decrease of 3°C and 5°C respectively; (2) an earlier deglacial initiation in the Antarctic Zone at 21 kyr B.P. than in the Subantarctic and Subtropical zones at ~16.5 kyr B.P.; (3) a concomitant deglacial ending in the three zones at around 14–14.5 kyr B.P.; (4) a decreasing Holocene SST trend in the Antarctic and Subantarctic zones for which no discernable equivalent exists in the Subtropical Zone; and (5) a 1-kyr phase between the two cooling events recorded in both the Antarctic Zone and the Subtropical Zone, highlighted by the shading in Figure 2. Beside these differences, a global glacial-interglacial pattern is consistent across the three cores showing a similar evolution of the isotherms up to the southern Subtropical Front (SSTF), and therefore a similar evolution of the physical environment in the studied area. However, the issue of shifting hydrological fronts in phase with isotherm development is still under debate, although there is growing evidence that the fronts are constrained to their modern positions by the bottom ocean topography throughout much of the Southern Ocean [*Moore et al.*, 1999; *Rintoul et al.*, 2001]. The surface isotherms representative of the modern northern Subtropical Front (NSTF) migrated much less than the surface isotherms representative of the modern Subantarctic Front (SAF) during the last glacial, indicating an expansion of the cold pool and a narrowing of the warm realm of the Southern Ocean [*Gersonde et al.*, 2003]. This in turn induced an intensification of the Antarctic Circumpolar Current, especially in the region of the Crozet-Kerguelen islands where the bottom topography strongly influences the circumpolar circulation [*Dézileau et al.*, 2000, 2003].

4.2. Isotopic and Elemental Ratios and Inferred Nutrient Cycling Changes

4.2.1. Rationale Behind the Isotopic and Elemental Ratios

[19] On a large scale, $\delta^{13}C$ is believed to primarily respond to the CO_2 concentration in surface waters [*Rau et al.*, 1989; *Popp et al.*, 1999; *Lourey et al.*, 2004] and plankton growth rate [*Rosenthal et al.*, 2000]. There is an inverse relationship between CO_{2aq} and $\delta^{13}C$ with depleted $\delta^{13}C$ values at high CO_2 concentrations, while there is a positive relationship between growth rate and $\delta^{13}C$ with enriched $\delta^{13}C$ values at high diatom growth rates. However, additional processes such as plankton cell size and shape [*Popp et al.*, 1998; *Burkhardt et al.*, 1999] and active carbon acquisition [*Cassar et al.*, 2004] can be important, especially in low-latitude upwelling systems [*Rau et al.*, 2001; *Tortell and Morel*, 2002]. The influence of plankton cell size/shape, however, is reduced when analyzing diatom-intrinsic organic matter in a given size fraction, <32 μm here. On a large scale, $\delta^{15}N$ is believed to record changes in nitrate relative utilization [*Altabet and François*, 1994], although plankton cell size and shape possibly blur the signal [*Karsh et al.*, 2003].

[20] In an ideal oceanic system, alleviation of iron limitation stimulates diatom growth rate and C and N uptake [*Takeda*, 1998; *Hutchins and Bruland*, 1998; *Brzezinski et al.*, 2002] leading to enriched $\delta^{13}C_{diat}$ and $\delta^{15}N_{diat}$ values. The Southern Ocean, however, is not an ideal oceanic system, particularly on glacial-interglacial timescales. Other factors such as sea ice dampening effect on productivity [*Burckle and Cirrili*, 1987] and migration of the isotherm-associated high productivity belt [*Burckle*, 1984] may counteract iron alleviation during glacial times. We therefore suggest that our elemental ratio records track iron-mediated C and N accumulation in DIOM and possibly in bulk diatoms, which is not necessarily dependent upon diatom growth rate. Our isotopic ratios represent a balance between positive factors (iron alleviation) and negative factors (sea ice and temperature changes, circulation changes) on diatom productivity.

4.2.2. Nutrient Cycling Changes

[21] Down-core records of C and N stable isotope ratios and elemental ratios in the two southern cores show a similar evolution during the last 50,000 years with lighter $\delta^{13}C_{diat}$ and heavier $\delta^{15}N_{diat}$ during the glacial period relative to the Holocene (Figure 3). This is in agreement with previous studies [*Singer and Shemesh*, 1995; *Crosta and Shemesh*, 2002; *Shemesh et al.*, 2002]. Carbon and nitrogen content also increased in both cores during the last glacial while C/N ratios decreased. Variations in the geochemical proxies seem related to climatic changes through the evolution of the isotherms at the core locations (Figure 2). In contrast to the southern cores, down-core records of $\delta^{13}C_{diat}$ and $\delta^{15}N_{diat}$ in the Subtropical core do not show the typical anti-correlation described at southern high latitudes [*Crosta and Shemesh*, 2002]. Similarly, they do not show any relationship with SST changes at the core site (Figure 3), while carbon and nitrogen content also display no glacial-interglacial changes. We therefore conclude that two major oceanic systems have prevailed in the Southern Ocean over the last 50,000 years: a first system composed of the Antarctic and Subantarctic zones, and a second system composed of the southern Subtropical zone.

4.2.3. Antarctic and Subantarctic Zones

[22] Biogenic silica content and authigenic uranium records indicate that the southern system is characterized, during glacial periods, by a shift of the high productivity belt by a few degrees of latitude to the north [*Anderson et al.*, 1998; *Bareille et al.*, 1998; *Asmus et al.*, 1999; *Chase et*

al., 2001; *Dézileau et al.*, 2003], hence following isotherm migration. The resulting lower productivity at the APF core site and greater productivity at the SAF core site during the last glacial should have led to different relative nutrient utilization and anti-correlated $\delta^{15}N_{diat}$ records in the absence of other processes. Correlated records from the two zones therefore imply here that an external factor is counterbalancing the requested depletion in the Antarctic $\delta^{15}N_{diat}$ record. Several hypotheses arise and can be tested according to our results.

[23] First, a northward migration of the upwelling along with the wind system and the isotherms would reduce nutrient input to Antarctic surface waters whilst increasing input to Subantarctic waters [*Sigman and Boyle*, 2000]. However, the APF serves as the northern boundary of wind-driven upwelling of deep-water. It is generally believed that the APF is fixed to its modern position through time because of a strong interaction with bottom topography, which hinders any possibility that upwelling could have been displaced to the north. Additionally, the glacial intensification of the wind system argues for higher eddy activity, preventing strong stratification of the surface waters [*Keeling and Visbeck*, 2001].

[24] Second, a shift in phytoplankton communities from siliceous to "non-skeletal" organic organisms in the Antarctic zone [*Anderson et al.*, 2002] would increase the global nutrient consumption and subsequently the $\delta^{15}N_{diat}$. This scenario is consistent with a fixed APF and a constant upwelling of deep-water. It is also consistent with the decoupling of organic carbon from biogenic silica accumulation in Southern Ocean sediments [*Anderson et al.*, 1998]. However, there is no geological evidence for increased deposition of organic carbon by "non-skeletal" organisms in glacial sediments because they are generally remineralized in the photic zone.

[25] Third, a glacial increase in NO_3^-:$Si(OH)_4$ consumption ratio and N_{org} to biogenic silica burial ratio (N_{org}:BSi) by diatoms would rapidly impoverish the nitrate pool, hence causing heavier $\delta^{15}N_{diat}$ [*Crosta et al.*, 2002]. Addition of iron into diatom cultures increases NO_3^-:$Si(OH)_4$ and CO_2aq:$Si(OH)_4$ uptake ratios [*Hutchins and Bruland*, 1998; *Takeda*, 1998]. High southern latitudes received 20–50 times more dust-bearing iron during glacial times [*Petit et al.*, 1999] from Patagonia [*Basile et al.*, 1997]. Additionally, iron transport which is today restricted to the Atlantic sector of the Southern Ocean was much more intense during the last glacial and was able to reach the Indian sector [*Andersen et al.*, 1998]. Although recent model experiments minimize the role of eolian iron compared to upwelled iron [*Lefevre and Watson*, 1999; *Archer and Johnson*, 2000], in situ observations demonstrate a direct response of seasonal phytoplankton stocks to seasonal dust deposition [*Erickson et al.*, 2003]. Moreover, in situ mesoscale experiments of iron fertilization in the Southern Ocean also produce a large response in the diatom community relative to other phytoplankton groups [*Boyd et al.*, 2000]. It is reasonable to think that glacial increase in dust-bearing iron influenced diatoms, promoting NO_3^- and CO_2aq consumption relative to $Si(OH)_4$, in relation to enhanced photosynthetic activity. In situ experiments in the equatorial Pacific indicate that phytoplankton responds to iron addition by enhancing their number and efficiency of photosystem II and then by increasing cellular chlorophyll [*Behrenfeld et al.*, 1996].

[26] However, only the export production to deep-sea environments affects the isotopic signals and atmospheric CO_2 concentrations. Labile organic matter that is remineralized in the photic zone regenerates nutrients and has little impact on the isotopic signals. The question is whether accumulation rates of refractory organic N and C were also changed by alleviation of the iron deficit during glacial times. Our SO136-111 records of N_{diat} and C_{diat} indicate more buried DIOM per unit of biogenic silica in the Antarctic zone during the last glacial than during the Early Holocene (Figure 3). Diatom-intrinsic organic matter is mainly composed of proteins [*Kröger and Sumper*, 1998] and is obviously more compound-specific than the bulk diatom, but it represents the major diatom organic material preserved in diatom ooze sediments [*Shemesh et al.*, 1993; *Sigman et al.*, 1999] because it is protected from remineralization by the frustule. The genetically controlled organic intrinsic template directs biosilica formation and frustule development [*Kröger et al.*, 1999; *Groß*, 2001]. The iron concentration in the medium that affects the degree of silicification of the frustules may similarly affect the composition of the DIOM. We therefore tentatively state that C_{diat} and N_{diat} evolution somehow parallels C_{org} and N_{org} evolution of bulk diatom because both evolutions are related to the same environmental conditions. This hypothesis obviously needs to be tested by concomitant analysis of DIOM and bulk organic matter through diatom culture experiments and determination of the elemental composition of the DIOM and its location through microprobes investigations. If these experiments support this hypothesis, then lower glacial productivity in the Antarctic Zone, caused by the presence of sea ice, may have been offset by increased storage of organic N as a result of iron fertilization. This process may have been the cause of the heavier glacial $\delta^{15}N_{diat}$ values. Sea ice presence and resulting lower diatom growth rates led to depleted glacial $\delta^{13}C_{diat}$ values despite increase in organic C storage. Lower productivity also implies less consumption of silicic acid and therefore depleted glacial δ^{30}Si values [*De La Rocha et al.*, 1998]. This third scenario alone explains the decoupling of organic carbon and biogenic silica accumulation rates in Southern Ocean sediments [*Anderson et al.*, 1998] and the anti-correlation of $\delta^{15}N_{diat}$ and δ^{30}Si in down-core records [*Brzezinski et al.*, 2002] while also being consistent with a constant nutrient input and a fixed APF.

[27] Heavier values of $\delta^{15}N_{diat}$ in core MD88-769 during the last glacial (Figure 3, SAF box) are consistent with greater productivity in the southern Subantarctic Zone during cold periods [*Anderson et al.*, 1998; *Bareille et al.*, 1998; *Asmus et al.*, 1999; *Chase et al.*, 2001; *Dézileau et al.*, 2003]. The two heaviest peaks are synchronous to the highest C_{diat} and N_{diat} (Figure 3, SAF box) and to the two coldest events at 22.7 kyr B.P. and 16.7 kyr B.P. (Figure 2, SAF box). The $\delta^{15}N_{diat}$ peaks therefore possibly result from

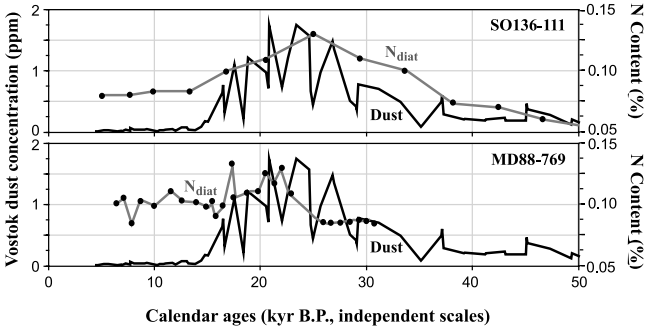

Figure 4. Comparison of Vostok dust concentration (black line) and N content of diatom-intrinsic organic matter from core SO136-111 (shaded curve, top box) and from core MD88-769 (shaded curve, lower box). The dust record and the marine records are plotted on independent timescales.

greater consumption and storage of C and N by diatoms in response to iron fertilization. Concomitant SST decreases and C_{diat} and N_{diat} peaks indicates that bio-available iron may have been transported to the core location by a more intense ACC or by cross-frontal diffusion when the cold Antarctic pool extent was maximized. Iron stimulation by direct eolian deposition is less plausible as the core is located at the extreme boundary of the glacial dust plume [*Andersen et al.*, 1998].

[28] Our data support the idea that iron availability might be a key element in the Indian sector of the Southern Ocean by modulating the NO_3^-:$Si(OH)_4$ and CO_2aq:$Si(OH)_4$ uptake ratios and N_{org}:BSi and C_{org}:BSi storage ratios by diatoms. Our third scenario is consistent with oceanographic data and reconciles all geochemical records.

4.2.4. Southern Subtropical Zone

[29] As demonstrated before, this zone represents a completely different system in which geochemical proxies do not co-vary with the glacial-interglacial SST record. Carbon-related proxies show no significant changes over the last 50 kyr B.P. and N-related proxies indicate a drop at 26 kyr B.P., largely out of phase with deglaciation (Figure 3, SSTF box). The down-core records cannot be explained by changes in siliceous productivity because opal rain rates in the southern Subtropical Zone are continuously low over the last 50 kyr B.P. [*Dézileau et al.*, 2003], which indicates that diatoms were never the main primary producers at the core site. The drop in $\delta^{15}N_{diat}$ and N_{diat} occurs when nitrate relative utilization is maximized in the high-latitude waters. If phytoplankton of the SSTF were feeding on waters transported from the Antarctic Zone to the Subtropical Zone by Ekman and eddy transports [*Park et al.*, 1993], then $\delta^{15}N_{diat}$ in core MD97-2101 should have been higher during the last glacial than during the Early Holocene. As the opposite situation is observed, we conclude that another nutrient source supported phytoplankton growth north of the SSTF. This source is probably the Indian Subtropical Gyre (ISG) the return branch of which is captured today by the northern part of the ACC [*Belkin and Gordon*, 1996]. We show here that a rather similar situation prevailed at the SSTF over the last 50 kyr B.P. Even during full glacial conditions when the Antarctic cold pool was greatly expanded and Ekman transport was greater due to more intense winds [*Klinck and Smith*, 1993], the Antarctic nutrient input was relatively low compared to the ISG source. The low Antarctic input may be due to consumption of the nutrients by phytoplankton from the Antarctic and Subantarctic zones before surface waters reached the SSTF and conversion of the northward moving surface waters into Subantarctic Mode Waters (SAMW) during winter cooling [*Belkin and Gordon*, 1996].

[30] Down-core records argue against SSTF migration because such a displacement by a few degrees of latitude would have placed the core under the influence of Antarctic waters or at least in the zone of SAMW formation, which would have been observed in the $\delta^{15}N_{diat}$ record.

[31] The lack of glacial-interglacial signal in the elemental ratios indicates that diatom physiology did not change significantly in the Indian Subtropical Zone. This also supports claims that this region was remote from dust deposition during the last 50 kyr B.P. [*Andersen et al.*, 1998].

4.2.5. Impact on Silicic Leakage From the Southern Ocean

[32] We provide here, for the first time, geochemical evidence that supports a potential remote action of the Southern Ocean through changes in the NO_3^-:$Si(OH)_4$ ratio of SAMW. The good agreement between dust flux recorded at Vostok [*Petit et al.*, 1999] and N_{diat} and C_{diat} for the southernmost core suggests a causal relationship (Figure 4, upper box). A similar relationship is observed for core MD88-769 from the Subantarctic Zone albeit with a weak response during the 27–23 kyr B.P. period when dust deposition was high (Figure 4, lower box). However, a question remains whether phytoplankton from the Subantarctic Zone was under the influence of direct dust input or water flow from the Antarctic Zone. In Antarctic and Subantarctic locations, we believe that iron fertilization, through dust deposition or water mixing, modified the photosynthetic activity of the diatoms toward greater uptake/storage of N and C and less uptake/storage of Si. This is true for both the Antarctic Zone where productivity was lower and the Subantarctic Zone where productivity was higher. Our northernmost down-core records indicate that the Subtropical Indian Zone was not influenced by southern surface waters. Southern surface waters sank to form SAMW before reaching the SSTF. If nutrients were not totally consumed to support higher Subantarctic productivity, then SAMW were enriched in $Si(OH)_4$ during glacial times. Antarctic diatoms, therefore, have the potential to modulate the productivity of remote oceanic regions by changing the nutrient content of the waters escaping from the Southern Ocean. However, the amount of NO_3^- and $Si(OH)_4$ in the SAMW is as important as the NO_3^-:$Si(OH)_4$ ratio. Waters having a low ratio ($Si(OH)_4 > NO_3^-$) but low nutrient content will have little impact on siliceous productivity in low latitudes. Variations of SAMW content and fluxes are still largely unknown on glacial-interglacial cycles. It is

essential to characterize such changes to determine whether the Southern Ocean regulates atmospheric pCO_2 variations.

5. Conclusion

[33] Carbon and nitrogen isotopic and elemental ratios analyzed in diatom-bound organic matter (DIOM) from three cores on a north-south transect (43°S to 57°S) allow nutrient cycling in the Indian sector of the Southern Ocean to be characterized over the last 50 kyr B.P. Isotopic ratios, when coupled to other geochemical proxies, argue for a northward migration of the high productivity zone during the last glacial period along with the expansion of the Antarctic Zone and associated high nutrient levels. The northward shift of the high productivity zone involved a movement of around 5° of latitude as it did not reach the location of the northernmost core. Elemental ratios indicate that iron might have influenced the diatom elemental stoichiometry on geological timescale as already shown by in situ experiments [*Boyd et al.*, 2000] and laboratory experiments [*Hutchins and Bruland*, 1998; *Takeda*, 1998; *Brzezinski et al.*, 2002]. During the last glacial period, alleviation of iron deficit by the high input of dust-bearing Fe [*Petit et al.*, 1999] resulted in greater uptake and accumulation of carbon and nitrogen in diatoms relative to silica in the two southern cores. DIOM elemental ratios from the northernmost core do not show a glacial-interglacial signal indicating that the southern Subtropical region was remote from direct dust deposition and northward advection of Fe-rich Antarctic surface waters during the investigated period because these waters sank as Subantarctic Mode Waters. It is suggested that subtropical phytoplankton instead fed on the nutrient poor waters of the Indian Subtropical Gyre.

[34] Antarctic diatoms have the potential to modulate the productivity of remote oceanic regions by changing the nutrient levels of the waters escaping from the Southern Ocean. Aside from drastic changes in Southern Ocean hydrology, higher NO_3^-:$Si(OH)_4$ and CO_2aq:-$Si(OH)_4$ uptake ratios by diatoms in the Polar Front Zone and Subantarctic Zone during the last glacial resulted in a greater concentration of silicic acid in Subantarctic Mode Waters, which represents the main source of nutrients for low-latitude upwelling systems [*Sarmiento et al.*, 2004].

[35] Changes in the Antarctic diatom nutrient uptake ratios have the potential to explain the observed decoupling between $\delta^{15}N$ and $\delta^{30}Si$ [*Brzezinski et al.*, 2002] and between accumulation rates of biogenic silica and organic carbon [*Anderson et al.*, 1998]. Higher NO_3^-:$Si(OH)_4$ uptake ratio by diatoms during the last glacial period resulted in heavier $\delta^{15}N$ and lighter $\delta^{30}Si$ than during interglacial periods because more nitrate was consumed relative to silicic acid. Similarly, higher C_{org}:BSi accumulation ratios in DIOM, and possibly bulk diatom, during the last glacial period led to greater sedimentary C_{org} content relative to biogenic silica. No shift in phytoplankton community is therefore needed to explain the observed decoupling in burial rates of C_{org} and biogenic silica [*Anderson et al.*, 2002].

[36] **Acknowledgments.** We thank Valérie Masson, Didier Paillard, Igor Belkin, and Huan-Yang Park for constructive discussions. We also thank two anonymous reviewers for helpful comments that improved the manuscript. Many thanks to George Swann and Eleanor Maddison for improving the Franglish. We personally thank people from TASQWA, APSARA, and IPHIS cruises. Financial support for this study was provided by CNRS (Centre national de la Recherche Scientifique), PNEDC (Programme national d'Etude de la Dynamique du Climat), and Missions Scientifiques des Terres Australes et Antarctiques Françaises (IPEV-TAAF). This is an EPOC contribution 1533.

References

Altabet, M. A., and R. François (1994), Sedimentary nitrogen isotopic ratio as a recorder for surface ocean nitrate utilization, *Global Biogeochem. Cycles*, *8*(1), 103–116.

Andersen, K. K., A. Armengaud, and C. Genthon (1998), Atmospheric dust under glacial and interglacial conditions, *Geophys. Res. Lett.*, *25*(13), 2281–2284.

Anderson, R. F., N. Kumar, R. A. Mortlock, P. N. Froelich, P. Kubik, B. Dittrich-Hannen, and M. Suter (1998), Late-Quaternary changes in productivity of the Southern Ocean, *J. Mar. Syst.*, *17*, 497–514.

Anderson, R. F., Z. Chase, M. Q. Fleisher, and J. Sachs (2002), The Southern Ocean's biological pump during the Last Glacial Maximum, *Deep Sea Res., Part II*, *49*, 1909–1938.

Archer, D. E., and K. Johnson (2000), A model of the iron in the ocean, *Global Biogeochem. Cycles*, *14*(1), 269–279.

Asmus, T., M. Frank, C. Koschmieder, N. Frank, R. Gersonde, G. Kuhn, and A. Mangini (1999), Variations of biogenic particle flux in the southern Atlantic section of the Subantarctic Zone during the late Quaternary: Evidence from sedimentary $^{231}Pa_{ex}$ and $^{230}Th_{ex}$, *Mar. Geol.*, *159*, 63–78.

Bard, E., M. Arnold, B. Hamelin, N. Tisnerat-Laborde, and G. Cabioch (1998), Radiocarbon calibration by means of mass spectrometric Th-^{230}/U-^{234} and C-^{14} ages of corals: An updated database including samples from Barbados, Mururoa and Tahiti, *Radiocarbon*, *40*(3), 1085–1092.

Bareille, G., M. Labracherie, P. Bertrand, L. Labeyrie, G. Lavaux, and M. Dignan (1998), Glacial-interglacial changes in the accumulation rates of major biogenic components in Southern Indian Ocean sediments, *J. Mar. Syst.*, *17*, 527–539.

Basile, I., F. E. Grousset, M. Revel, J. B. Petit, P. E. Biscaye, and N. I. Barkov (1997), Patagonian origin of glacial dust deposited in East Antarctica (Vostok, Dome C) during glacial stages 2, 4 and 6, *Earth Planet. Sci. Lett.*, *146*(3-4), 573–590.

Behrenfeld, M. J., A. J. Bale, Z. S. Kolber, J. Aiken, and P. G. Falkowski (1996), Confirmation of iron limitation of phytoplankton photosynthesis in the equatorial Pacific Ocean, *Nature*, *383*, 508–511.

Belkin, I. M., and A. L. Gordon (1996), Southern Ocean fronts from the Greenwich meridian to Tasmania, *J. Geophys. Res.*, *101*(C2), 3675–3696.

Boyd, P. W., et al. (2000), A mesoscale phytoplankton bloom in the polar Southern Ocean stimulated by iron fertilization, *Nature*, *407*, 695–702.

Brzezinski, M. A., C. J. Pride, V. Franck, D. M. Sigman, J. L. Sarmiento, K. Matsumoto, N. Gruber, G. H. Rau, and K. H. Coale (2002), A switch from $Si(OH)_4$ to NO_3^- depletion in the glacial Southern Ocean, *Geophys. Res. Lett.*, *29*(12), 1564, doi:10.1029/2001GL014349.

Burckle, L. H. (1984), Diatom distribution and paleoceanographic reconstruction in the Southern Ocean–Present and Last Glacial Maximum, *Mar. Micropaleontol.*, *9*, 241–261.

Burckle, L. H., and J. Cirrili (1987), Origin of the diatom ooze belt in the Southern Ocean: Implications for the late Quaternary paleoceanography, *Micropaleontology*, *33*(1), 82–86.

Burkhardt, S., U. Riebesell, and I. Zondervan (1999), Effects of growth rate, CO_2 concentration, and cell size on the stable carbon isotope fractionation in marine phytoplankton, *Geochim. Cosmochim. Acta*, *63*(22), 3729–3741.

Cassar, N., E. A. Laws, and R. R. Bidigare (2004), Bicarbonate uptake by Southern Ocean phytoplankton, *Global Biogeochem. Cycles*, *18*, GB2003, doi:10.1029/2003GB002116.

Chase, Z., R. F. Anderson, and M. Q. Fleisher (2001), Evidence from authigenic uranium for increased productivity of the glacial Subantarctic Ocean, *Paleoceanography*, *16*(5), 467–478.

Crosta, X., and A. Shemesh (2002), Reconciling down-core anti-correlation of diatom carbon and nitrogen isotopic ratios from the Southern Ocean, *Paleoceanography*, *17*(1), 1010, doi:10.1029/2000PA000565.

Crosta, X., A. Shemesh, M. E. Salvignac, H. Gildor, and R. Yam (2002), Late Quaternary variations of elemental ratios (C:Si and N:Si) in diatom-bound organic matter from the Southern Ocean, *Deep Sea Res., Part II*, *49*, 1939–1952.

Crosta, X., A. Sturm, L. Armand, and J. J. Pichon (2004), Late Quaternary sea ice history in the Indian sector of the Southern Ocean as recorded by diatom assemblages, *Mar. Micropaleontol.*, *50*, 209–223.

De la Rocha, C. L., M. A. Brzezinski, M. J. DeNiro, and A. Shemesh (1998), Silicon-isotope composition of diatom as an indicator of past oceanic change, *Nature*, *395*, 680–683.

Dézileau, L., G. Bareille, J. L. Reiss, and F. Lemoine (2000), Evidence for strong sediment redistribution by bottom currents along the southeast Indian Ridge, *Deep Sea Res., Part I*, *47*, 1899–1936.

Dézileau, L., J. L. Reyss, and F. Lemoine (2003), Late Quaternary changes in biogenic opal fluxes in the Southern Indian Ocean, *Mar. Geol.*, *202*, 143–158.

Erickson, D. J., J. L. Hernandez, P. Ginoux, W. W. Gregg, C. McClain, and J. Christian (2003), Atmospheric iron delivery and surface ocean biological activity in the Southern Ocean and Patagonian region, *Geophys. Res. Lett.*, *30*(12), 1609, doi:10.1029/2003GL017241.

François, R., M. A. Altabet, E. F. Yu, D. M. Sigman, M. P. Bacon, M. Frank, G. Bohrmann, G. Bareille, and L. D. Labeyrie (1997), Contribution of Southern Ocean surface-water stratification to low atmospheric CO_2 concentrations during the last glacial period, *Nature*, *389*, 929–935.

Gersonde, R., et al. (2003), Last glacial sea surface temperatures and sea-ice extent in the Southern Ocean (Atlantic-Indian sector): A multi-proxy approach, *Paleoceanography*, *18*(3), 1061, doi:10.1029/2002PA000809.

Groß, M. (2001), Les nanotechnologies et le plancton, *Recherche*, *338*, 20–21.

Hutchins, D. A., and K. W. Bruland (1998), Iron-limited diatoms growth and Si:N uptake ratios in a coastal upwelling regime, *Nature*, *393*, 561–564.

Karsh, K. L., T. W. Trull, M. J. Lourey, and D. M. Sigman (2003), Relationship of nitrogen isotope fractionation to phytoplankton size and iron availability during the Southern Ocean Iron RElease Experiment (SOIREE), *Limnol. Oceanogr.*, *48*(3), 1058–1068.

Keeling, R. F., and B. B. Stephens (2001), Antarctic sea ice and the control of Pleistocene climate instability, *Paleoceanography*, *16*(1), 112–131.

Keeling, R. F., and M. Visbeck (2001), Antarctic stratification and glacial CO_2, *Nature*, *412*, 605–606.

Klinck, J. M., and D. A. Smith (1993), Effect of wind changes during the Last Glacial Maximum on the circulation in the Southern Ocean, *Paleoceanography*, *8*(4), 427–433.

Kröger, N., and M. Sumper (1998), Diatom cell wall proteins and the cell biology of silica biomineralization, *Protist*, *149*, 213–219.

Kröger, N., R. Deutzmann, and M. Sumper (1999), Polycationic peptides from diatom biosilica that direct silica nanosphere formation, *Science*, *286*, 1129–1132.

Kumar, N., R. F. Anderson, R. A. Mortlock, P. N. Froelich, P. Kubik, B. Dittrich-Hannen, and M. Suter (1995), Increased biological productivity and export production in the glacial Southern Ocean, *Nature*, *378*, 675–680.

Laws, R. A. (1983), Preparing strewn slides for quantitative microscopical analysis: A test using calibrated microspheres, *Micropaleontology*, *24*, 60–65.

Lefevre, N., and A. J. Watson (1999), Modelling the geochemical cycle of iron in the oceans and its impact on atmospheric CO_2 concentrations, *Global Biogeochem. Cycles*, *13*(3), 727–736.

Levitus, S. (1994), *World Ocean Atlas* [CD-ROM], vol. 1, *Temperature*, Natl. Oceanic and Atmos. Admin., Silver Spring, Md.

Lourey, M. J., T. W. Trull, and B. Tilbrook (2004), Sensitivity of $\delta^{13}C$ of Southern Ocean suspended and sinking organic matter to temperature, nutrient utilization, and atmospheric CO_2, *Deep Sea Res., Part I*, *51*, 281–305.

Matsumoto, K., J. L. Sarmiento, and M. A. Brzezinski (2002), Silicic acid leakage from the Southern Ocean: A possible explanation for glacial atmospheric pCO_2, *Global Biogeochem. Cycles*, *16*(3), 1031, doi:10.1029/2001GB001442.

Moore, J. K., M. R. Abbott, and J. G. Richman (1999), Location and dynamics of the Antarctic Polar Front from satellite sea-surface temperature data, *J. Geophys. Res.*, *104*(C2), 3059–3073.

Naval Oceanography Command Detachment (1985), *Sea Ice Climatic Atlas*, vol. 1, *Antarctic*, Commander, Nav. Oceanogr. Command, Asheville, N. C.

Paillard, D., L. Labeyrie, and P. Yiou (1996), Macintosh program performs time-series analysis, *Eos Trans. AGU*, *77*, 379.

Park, Y. H., L. Gamberoni, and E. Charriaud (1993), Frontal structure, water masses and circulation in the Crozet Basin, *J. Geophys. Res.*, *98*(7), 12,361–12,385.

Petit, J. R., et al. (1999), Climate and atmospheric history of the past 420.000 years from the Vostok ice core, Antarctica, *Nature*, *399*, 429–436.

Popp, B. N., E. A. Laws, R. R. Bidigare, J. E. Dore, K. L. Hanson, and S. G. Wakeham (1998), Effect of phytoplankton cell geometry on carbon isotopic fractionation, *Geochim. Cosmochim. Acta*, *62*(1), 69–77.

Popp, B. N., et al. (1999), Controls on the carbon isotopic composition of Southern Ocean phytoplankton, *Global Biogeochem. Cycles*, *13*(4), 827–843.

Rathburn, A. E., J. J. Pichon, M. A. Ayress, and P. DeDeckker (1997), Microfossil and stable-isotope evidence for changes in Late Holocene paleoproductivity and paleoceanographic conditions in the Prydz Bay region of Antarctica, *Paleogeogr. Paleoclimatol. Paleoecol.*, *131*, 485–510.

Rau, G. H., T. Takahashi, and D. J. Des Marais (1989), Latitudinal variations in plankton $\delta^{13}C$: Implications for CO_2 and productivity in past oceans, *Nature*, *341*, 516–518.

Rau, G. H., F. P. Chavez, and G. E. Freiderich (2001), Plankton $^{13}C/^{12}C$ variations in Monterey Bay, California: Evidence of non-diffusive inorganic carbon uptake by phytoplankton in an upwelling environment, *Deep Sea Res., Part I*, *48*, 79–94.

Rintoul, S. R., C. W. Hughes, and D. Olbers (2001), The Antarctic Circumpolar Current, in *Ocean Circulation and Climate: Observing and Modelling the Global Ocean*, edited by G. Siedler et al., pp. 271–302, Elsevier, New York.

Robinson, R. S., B. G. Brunelle, and D. M. Sigman (2004), Revisiting nutrient utilization in the glacial Antarctic: Evidence from a new method for diatom-bound N isotopic analysis, *Paleoceanography*, *19*, PA3001, doi:10.1029/2003PA000996.

Rosenthal, Y., M. Dahan, and A. Shemesh (2000), The glacial Southern Ocean: A source of atmospheric CO_2 as inferred from carbon isotopes in diatoms, *Paleoceanography*, *15*(1), 65–75.

Sarmiento, J. L., M. Gruber, M. A. Brzezinski, and J. P. Dunne (2004), High-latitude controls of thermocline nutrients and low latitude biological productivity, *Nature*, *427*, 56–60.

Schmittner, A. (2003), Southern Ocean sea ice and radiocarbon ages of glacial bottom waters, *Earth Planet. Sci. Lett.*, *213*(1-2), 53–62.

Schrader, H. J., and R. Gersonde (1978), Diatoms and silicoflagellates, *Utrecht Micropaleontol. Bull.*, *17*, 129–176.

Shemesh, A., S. A. Macko, C. D. Charles, and G. H. Rau (1993), Isotopic evidence for reduced productivity in the glacial Southern Ocean, *Science*, *262*, 407–410.

Shemesh, A., D. Hodell, X. Crosta, S. Kanfoush, C. Charles, and T. Guilderson (2002), Sequence of events during the last deglaciation in Southern Ocean sediments and Antarctic ice cores, *Paleoceanography*, *17*(4), 1056, doi:10.1029/2000PA000599.

Sigman, D. M., and E. A. Boyle (2000), Glacial/interglacial variations in atmospheric carbon dioxide, *Nature*, *407*, 859–869.

Sigman, D. M., M. A. Altabet, R. Francois, D. C. McCorkle, and J. F. Gaillard (1999), The isotopic composition of diatom-bound nitrogen in the Southern Ocean sediments, *Paleoceanography*, *14*(2), 118–134.

Singer, A. J., and A. Shemesh (1995), Climatically linked carbon isotope variation during the past 430,000 years in Southern Ocean Sediments, *Paleoceanography*, *10*(2), 171–177.

Stephens, B. B., and R. F. Keeling (2000), The influence of Antarctic sea ice on glacial-interglacial CO_2 variations, *Nature*, *404*, 171–174.

Stuivert, M., P. J. Reimer, and T. F. Braziunas (1998), High-precision radiocarbon age calibration for terrestrial and marine samples, *Radiocarbon*, *40*(3), 1127–1151.

Takeda, S. (1998), Influence of iron availability on nutrients consumption ratio of diatoms in oceanic waters, *Nature*, *393*, 774–777.

Toggweiler, J. R. (1999), Variation of atmospheric CO_2 by ventilation of the ocean's deepest water, *Paleoceanography*, *14*(5), 571–588.

Tortell, P. D., and F. M. M. Morel (2002), Sources of inorganic carbon for phytoplankton in the eastern Subtropical and Equatorial Pacific Ocean, *Limnol. Oceanogr.*, *47*(4), 1012–1022.

van Beek, P., J. L. Reyss, M. Paterne, R. Gersonde, M. R. van der Loeff, and G. Khun (2002), ^{226}Ra in barite: Absolute dating of Holocene Southern Ocean sediments and reconstruction of sea-surface reservoir ages, *Geology*, *30*(8), 731–734.

I. Billy, X. Crosta, and J. Etourneau, Département de Géologie et Océanographie (DGO), UMR-CNRS 5805 EPOC, Université Bordeaux I, Avenue des facultés, 33405 Talence, France. (x.crosta@epoc.u-bordeaux1.fr)

A. Shemesh and R. Yam, Environmental Sciences and Energy Research, Weizmann Institute of Science, 76100 Rehovot, Israel.